Journal of Applied Mechanics and Technical Physics, Vol. 36, No. 1, 1995

PRESSURE WAVES IN A LIQUID SUSPENSION WITH SOLID PARTICLES AND GAS BUBBLES

V. E. Dontsov, V. E. Nakoryakov, and B. G. Pokusaev

UDC 532.529

The propagation of pressure disturbances in a suspension of a liquid and solid particles is a subject that has been studied quite extensively. The theory of multiple scattering was used in [1, 2] to obtain expressions for the velocity and attenuation factor of an acoustic wave, and the results were compared with experimental data. Good agreement between theoretical and experimental data on the speed and attenuation of sound in suspensions was obtained in [3] on the basis of the Biot model for the propagation of sound in saturated porous media. The author of [4] presented averaged equations of the mechanics of disperse media that make it possible to examine the evolution of waves in two-phase mixtures. The results of a series of theoretical and experimental studies on wave dynamics in gas-liquid media were presented in [5], and the propagation of waves in porous media saturated with a gas–liquid mixture was examined in [6].

Our goal here is to experimentally study the evolution and structure of pressure waves of moderate intensity in a suspension of a liquid with solid particles and gas bubbles. We also want to generalize the empirical data on the basis of a theoretical analysis.

We will examine the propagation of unidimensional pressure disturbances in a liquid containing suspended solid spheres and gas bubbles. We assume that the length of the waves associated with the disturbances is much greater on the dimensions of the spheres, the dimensions of the bubbles, and the distances between them. We represent a liquid with gas bubbles as a homogeneous medium having the mean density ρ_m, pressure p, and velocity v_m. For a disperse medium (solid spheres + homogeneous gas–liquid medium), the system of equations describing the propagation of unidimensional pressure perturbations has the form [4]

$$\frac{\partial m\rho_m}{\partial t}+\frac{\partial(m\rho_m v_m)}{\partial x}=0,\ \frac{\partial(1-m)\rho_1}{\partial t}+\frac{\partial(1-m)\rho_1 v_1}{\partial x}=0,$$
$$\alpha m\rho_m\frac{dv_m}{dt}-(\alpha-1)\,m\rho_m\frac{\partial v_1}{\partial t}=-m\frac{\partial p}{\partial x}-F_v, \tag{1}$$
$$-(\alpha-1)\,m\rho_m\frac{dv_m}{dt}+((1-m)\rho_1+(\alpha-1)\,m\rho_m)\frac{\partial v_1}{\partial t}$$
$$=-(1-m)\frac{\partial p}{\partial x}+F_v,\ \rho_1=\text{const},$$

where $\rho_m = \rho_2(1-\varphi)+\rho_3\varphi$; m is the porosity of the medium; φ is the volumetric gas content of the liquid (thus, the quantity φm will correspond to the volumetric gas content in the three-phase medium at low values of φ); α is a coefficient expressing the apparent additional mass of the liquid. The subscripts 1, 2, and 3 pertain to the solid, liquid, and gas phases, m pertains to the gas–liquid mixture, and 0 denotes the initial state of a phase.

We represent the interfacial force F_v as [4]

$$F_v=\frac{3}{4}\frac{c_v\rho_m m(1-m)(v_m-v_1)^2}{d}.$$

Here, d is the diameter of the solid spheres; c_v is the resistance coefficient, determined experimentally. At low relative velocities, the interfacial force depends linearly on relative velocity:

Novosibirsk. Translated from Prikladnaya Mekhanika i Tekhnicheskaya Fizika, No. 1, pp. 32-40, January-February, 1995. Original article submitted March 11, 1995.

0021-8944/95/3601-0030$12.50

$$F_v = \frac{m^2 \nu \rho_m}{K_0}(v_m - v_1)$$

(K_0 is permeability, usually introduced for porous media).

To close system (1), we obtain the relationship between the pressure p and the density of the homogeneous mixture ρ_m by using an equation to express the pulsations of a single bubble in a liquid with suspended solid particles. We will examine two limiting cases for oscillations of the bubble. In one case, when there is no radial motion between the liquid and the solid particles, i.e., when the particles are frozen in the liquid, we obtain the Rayleigh equation for pulsations of a bubble in an effective liquid with the density $\rho_0 = \rho_1(1 - m) + \rho_2 m$. This approach is valid when the densities of the solid and liquid phases are close to one another or when the period of oscillation of the bubbles is much longer than the time it takes for liquid boundary layers to form on the solid spheres.

Following [5] and changing over from the radius of the bubble to the density of the three-phase medium $\rho(\rho = \rho_0(1 - m\varphi) + \rho_3 m\varphi)$, we obtain

$$\delta\left(\rho - \frac{p}{c_w^2}\right) = -\frac{1}{c_w^2}\left(\bar{\beta}\frac{\partial^2 \rho}{\partial t^2} + \frac{4\bar{\nu}}{3\varphi m}\frac{\partial \rho}{\partial t} + \bar{B}c_w^2(\delta\rho)^2\right), \tag{2}$$

where $c_W = (\gamma p/\rho\varphi m)^{1/2}$ is the Wood velocity for a three-phase medium; $\bar{\beta} = R_0^2/3\varphi m$ is the dispersion coefficient; $\bar{B} = (\gamma + 1)/2\rho\varphi m$ is the coefficient of nonlinearity; R_0 is the radius of a bubble; $\bar{\nu}$ is the effective viscosity of the suspension of liquid and solid particles; γ is the adiabatic exponent.

In the other limiting case, when the densities of the liquid and particles differ significantly and the frequency of bubble oscillation is relatively high ($\omega >> \omega_m = m\nu/20K_0$ [7]), there is not enough time for the particles to undergo radial oscillations about the bubble. In this case, the equation for the oscillations of the bubble are obtained in the same manner as the equation for the oscillation of a bubble in a saturated incompressible porous medium [7]. Changing over from the bubble radius to ρ_m, we have

$$\delta\left(\rho_m - \frac{p}{c_0^2}\right) = -\frac{1}{c_0^2}\left(\beta\frac{\partial^2 \rho_m}{\partial t^2} + \frac{4\nu^*}{3\varphi}\frac{\partial \rho_m}{\partial t} + Bc_0^2(\delta\rho_m)^2\right). \tag{3}$$

Here, $c_0 = (\gamma p_0/\rho_m\varphi)^{1/2}$ is low-frequency sonic velocity in the gas–liquid mixture; $\beta = R_0^2/3\varphi$; $B = (\gamma + 1)/2\rho_m\varphi$; $\nu^* = \nu(1 + mR_0^2/4K_0) + \nu_T$; ν is the kinematic viscosity of the liquid; $\nu_T = (\gamma - 1)R_0\sqrt{\omega_0 a}/(\sqrt{2\varphi})$ is the coefficient of effective thermal viscosity [5]; ω_0 is the resonance frequency of oscillation of the bubbles; a is the diffusivity of the gas.

We can use closed system (1), (3) to obtain an evolutionary equation for pressure p, with the assumption that the nonlinear, dispersive, and dissipative terms are small. Since the nonlinearity in Eq. (3) is considerably greater than the hydrodynamic nonlinearity in Eqs. (1), we can linearize system (1). If we assume that the interfacial force at the liquid–solid boundary is linearly dependent on relative velocity and if we take into account the unsteady Basse force [4], we can reduce system (1) to the equation

$$\frac{\partial^2 \rho_m}{\partial t^2} - \left(\frac{c}{c_0}\right)^2 \frac{\partial^2 p}{\partial x^2} + \frac{m\nu}{K_0}\frac{m(1 - m)\rho_1 - ((c_0/c)^2 - m^2)\rho_m}{\alpha m(1 - m)\rho_1 + (\alpha - 1)m^2\rho_m} \times \left(\frac{\partial \rho_m}{\partial t} + \frac{1}{\sqrt{2\pi}\sqrt{m\nu/20K_0}}\int_0^t \frac{\partial \rho_m}{\partial \tau}\frac{d\tau}{\sqrt{t - \tau}}\right) = 0, \tag{4}$$

where

$$c = c_0\left(\frac{(\alpha - 2m + m^2)\rho_m + m(1 - m)\rho_1}{\alpha m(1 - m)\rho_1 + (\alpha - 1)m^2\rho_m}\right)^{1/2}$$

is sonic velocity in the three-phase mixture.

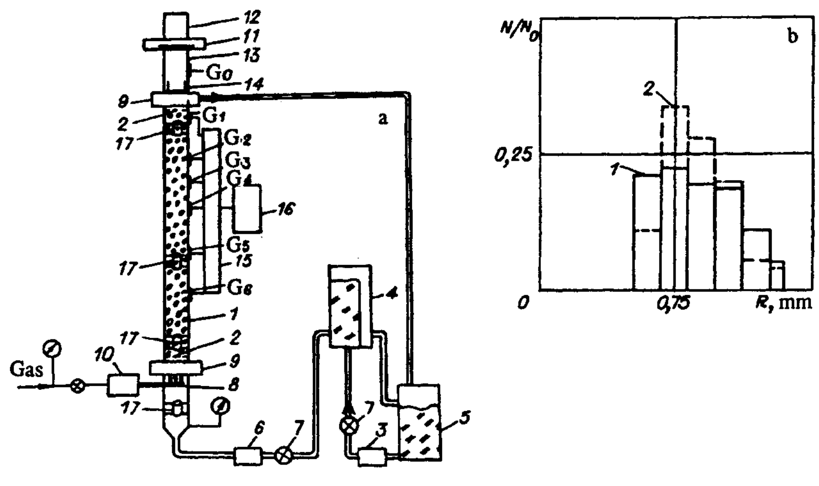

Fig. 1

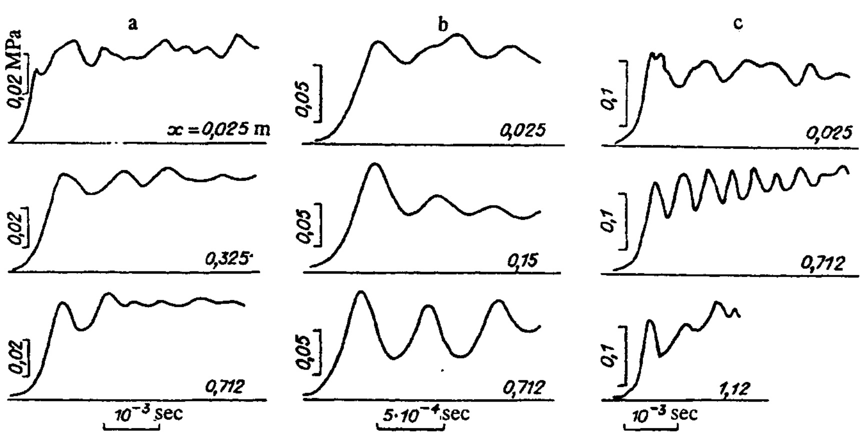

Fig. 2

If we further assume that the nonlinear, dispersive, and dissipative terms are small and we substitute $\delta\rho_m = \delta p/c_0^2$ into them, we obtain the following evolutionary equation from (3-4)

$$\frac{\partial^2 p}{\partial t^2} - c^2 \frac{\partial^2 p}{\partial x^2} + \frac{m\nu}{K_0} \frac{m(1-m)\rho_1 - ((c_0/c)^2 - m^2)\rho_m}{\alpha m(1-m)\rho_1 + (\alpha - 1)m^2\rho_m}$$
$$\times \left(\frac{\partial p}{\partial t} + \frac{1}{\sqrt{2\pi m\nu/20K_0}} \int_0^t \frac{\partial p}{\partial \tau} \frac{d\tau}{\sqrt{t-\tau}}\right) - \left(\frac{c}{c_0}\right)^2 \left(\beta \frac{\partial^4 p}{\partial x^2 \partial t^2} + \frac{4\nu^*}{3\varphi} \frac{\partial^3 p}{\partial x^2 \partial t} + B \frac{\partial^2 (\delta p)^2}{\partial x^2}\right) = 0. \tag{5}$$

If we ignore the apparent additional mass of the liquid, the expression for sonic velocity will have the form

$$c\big|_{\alpha=1} = \left(\frac{\gamma p_0}{\rho_c \varphi}\left(1 + \frac{1-m}{m}\frac{\rho_c}{\rho_1}\right)\right)^{1/2}.$$

This equation differs from the Navier—Stokes—Boussinesq equation for bubbly systems in the presence of an additional term accounting for viscous dissipation due to relative longitudinal displacement of the liquid and particles in the wave. If we ignore dissipation due to the relative longitudinal displacement in (5), we find a solution in the form of a shock wave having the velocity

$$\frac{U}{c} = \left(1 + \frac{\gamma + 1}{2\gamma}\frac{\delta p}{p_0}\right)^{1/2}. \tag{6}$$

If we ignore all dissipative losses in (5), we obtain the Boussinesq equation. Solitons are among the steady-state solutions of this equation. The expressions for the velocity and half-width of a soliton have the form

$$\frac{U_m}{c} = \left(1 + \frac{\gamma + 1}{3\gamma}\frac{\delta p_e}{p_0}\right)^{1/2}, \delta_t = \left(\beta\left(4 + \frac{12p_0}{\delta p_e}\frac{\gamma}{\gamma + 1}\right)\right)^{1/2}\left(\frac{c}{c_0}\right). \tag{7}$$

In the other limiting case, we can use system (1-2) to obtain the evolutionary equation

$$\frac{\partial^2 p}{\partial t^2} - c_w^2\frac{\partial^2 p}{\partial x^2} - \bar{\beta}\frac{\partial^4 p}{\partial x^2 \partial t^2} - \frac{4\bar{\nu}}{3\varphi m}\frac{\partial^3 p}{\partial x^2 \partial t} - \bar{B}\frac{\partial^2(\delta p)^2}{\partial x^2} = 0. \tag{8}$$

If we ignore dissipative losses, we obtain a steady-state solution — solitons:

$$\Delta p = \delta p_e \mathrm{sech}^2\left(\frac{x}{\delta_t}\right), \delta_t = \left(\bar{\beta}\left(4 + \frac{12p_0}{\delta p_e}\frac{\gamma}{\gamma + 1}\right)\right)^{1/2}. \tag{9}$$

In order to study the propagation of pressure waves in three-phase media (liquid — suspended solid particles — gas bubbles), we built the unit depicted in Fig. 1a. The working section 1 was a vertical thick-walled steel tube with an inside diameter of 52 mm and a length of 1.5 m. The tube was partially filled with glass spheres 3 mm in diameter. Grids 2 with a mesh of 2.5 mm were placed at the top and bottom of the tube. The porosity of the medium was determined from the volume of the working section and the volume of the spheres placed inside it.

To weigh the solid particles, liquid was pumped through the working section at a constant rate. Here, we used a constant-level system consisting of a pump 3, a constant-level tank 4, a drain tank 5, an inductance-type flow meter 6, and control valves 7. As the working medium, we used tap water and a solution of water and glycerin. Gas bubbles were introduced into the lower part of the working chamber by means of a needle-type bubble generator 8. Air and helium were used as the gases.

Figure 1b presents a histogram showing the size distribution of the air bubbles for two values of gas content. In the figure, 1 corresponds to $\varphi = 2.3\%$ and 2 corresponds to $\varphi = 0.85\ \%$. Transparent windows 9 were provided in the upper and lower parts of the working section to permit photographing of the bubbles. Low gas flow rates were measured by using a differential manometer to measure the pressure gradient over a long thin capillary built into the gas supply system. The gas flow meter 10 and the instrument used to measure liquid flow rate were calibrated before the experiments.

A stepped pressure wave was created by the rupture of diaphragm 11 separating the high-pressure chamber 12 from the low-pressure chamber 13. This wave was then propagated to the working section by the movement of lightweight piston 14. Piezoelectric pressure gages D were used to measure the profiles of the pressure waves. The gages were embedded in the wall along the working section so that they were flush with the section's inside surface. Signals from the gages were sent to analog-to-digital converter 15 and then analyzed by computer 16.

Low volumetric gas contents in the three-phase medium were measured with annular conduction gages 17. These gages were placed in the lower, middle, and upper parts of the working section. The effects of temperature and the salinity of the water were alleviated by using a reference conduction gage (positioned ahead of the working section) and a bridge circuit. The latter connected the measuring and reference gages to one another and operated at a frequency of 1 kHz. The conduction gages were calibrated in a two-phase (liquid — suspended solid particles) medium by making small changes in porosity (1-5% of the working value m_0).

The results of the calibration were used to construct the dependence of the relative change in porosity $\delta m/m_0$ on the average unbalance of the bridge. We obtained the dependence of gas flow rate on the average unbalance for the indicated working value of porosity m_0 in a three-phase medium (gas bubbles — liquid — solid spheres). We then constructed a calibration curve for the dependence of gas content $\varphi = -\delta m/m_0$ on gas flow rate at the value of m_0 used in the experiment.

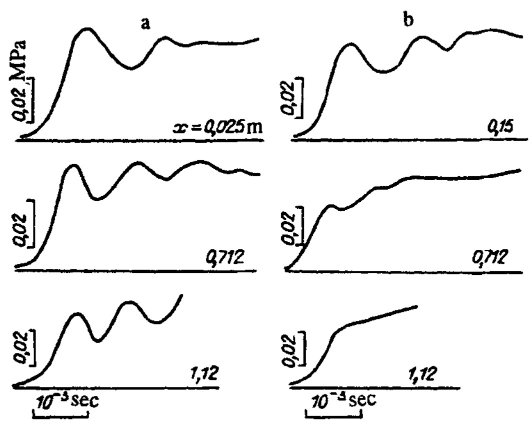

Fig. 3

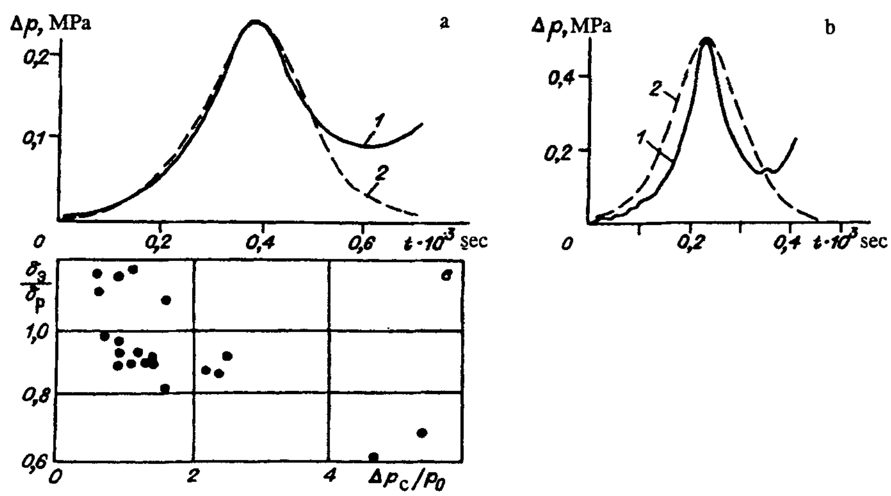

Fig. 4

The advantage of this method of calibration is the possibility of measuring relatively low volumetric gas contents ($\varphi \lesssim 1\%$) by linear approximation of the calibration curve to zero.

The tests showed that nonlinear and dispersive effects caused by radial vibrations of bubbles in the wave have a significant influence on the propagation of the wave in the suspension. Figure 2 shows the evolution of the wave in water with glass spheres and air bubbles for different volumetric gas contents φ and wave intensities Δp [where x is the distance from the point where the wave enters the medium to the measurement point, with the parameters of the medium being $m = 0.58$ and $\varphi = 0.5\%$ (a, b) and 2.3% (c)]. It is evident that the dispersive and nonlinear effects are weak and have almost no influence on the shape of the wave for low values of φ and low-amplitude waves. In this case, there is not enough time for an oscillating shock wave to form at the distances we investigated (Fig. 2a).

A quasisteady oscillating shock wave is formed at $x = 0.712$ m with an increase in wave amplitude to $\Delta p/p_0 = 0.7$. Dissipative processes cause the wave to attenuate slowly as it propagates (Fig. 2b). With an increase in volumetric gas content, dissipation leads to the appearance of a relaxation zone on the leading edge of the wave and damping of the oscillations (Fig. 2c).

Comparing the pressure-wave profiles with data on the propagation of pressure waves in gas–liquid media [5], we find that they agree qualitatively. Thus, the introduction of a solid phase into a gas–liquid medium does not qualitatively alter the dynamics of the wave but does produce quantitative changes in its velocity and structure. The solutions of Eqs. (5) and (8) can be used to more accurately describe the evolution of waves in three-phase media.

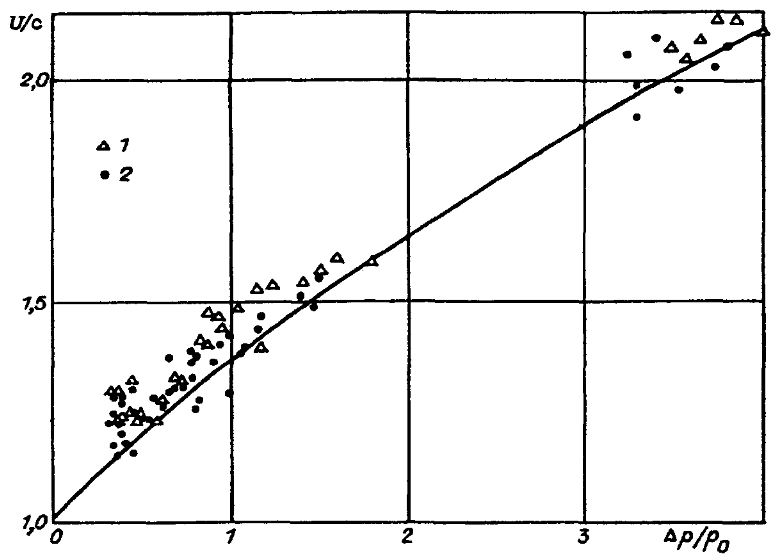

Fig. 5

To study the mechanisms by which the attenuation of pressure waves takes place in a three-phase medium, we conducted tests using water and a water-glycerin solution with a viscosity $\nu = 3 \cdot 10^{-6}$ m^2/sec as the liquid. We also used gases with different diffusivities. It was found that if the remaining parameters of the medium and wave are the same, there is no significant difference between the evolution of pressure waves in water with solid spheres and air bubbles and the evolution of such waves in a similar system with a water-glycerin solution as the liquid. At the same time, a change in the diffusivity of the gas in the bubbles appreciably alters the dissipative properties of the medium.

Figure 3 shows the evolution of pressure waves in a suspension of water with solid spheres and bubbles of air (a) and helium (b). The parameters of the medium and the wave were otherwise similar ($m = 0.58$, $\varphi = 1.4\%$). It is evident that a change in the coefficient of effective thermal viscosity ν_T changes the structure of the wave by a factor of nearly three. An oscillating shock wave is formed in Fig. 3a, but dissipative effects lead only to the appearance of the relaxation zone. At the same time, Fig. 3b shows that a monotonic pressure profile is formed from the initial signal due to strong dissipation. The formation of such a profile is connected with an increase in heat transfer between the gas in the bubbles and the surrounding liquid. This means that, as in gas–liquid media, the main mechanism responsible for wave dissipation in three-phase suspensions is heat dissipation.

Studies of the structure of weakly nonlinear shock waves have shown that the first oscillation of the wave is described well by a soliton. Lines 1 and 2 in Fig. 4, respectively, compare the form of the first oscillation of a shock wave and the result calculated from (9). For wave amplitudes $\Delta p_e/p_0 \sim 1$, the experimental profile is described well by the theoretical curve 2 (Fig. 4a), which makes no allowance for the relative radial motion of the liquid and solid particles around bubbles in the wave. Thus, even for solid particles with a relatively high density ($\rho_1/\rho_2 = 2.46$), the dispersive properties of the three-phase medium are practically no different than the dispersive properties of a gas–liquid medium. The dispersion coefficient of the medium is determined by the volumetric gas content φm and has the form $\beta = R_0^2/3\varphi m$.

An increase in the amplitude of the shock wave is accompanied by a substantial decrease in the duration of the oscillations and an increase in their acuity. The experimental profile of the first oscillation in a wave with the amplitude $\Delta p_e/p_0 = 4.7$ differs significantly from the form of the theoretical soliton (Fig. 4b).

Figure 4c compares the half-width of the first experimental wave oscillation δ_e and the theoretical value δ_t for $\varphi = 0.5 + 0.9\%$ ($\delta_e = t^*U$, where t^* is the time over which pressure in the front increases from $0.42\Delta p_e$ to Δp_e, Δp_e being the amplitude of the first oscillation and U the velocity of the shock wave). For amplitudes $\Delta p_e/p_0 \lesssim 2$, the half-width of the first oscillation of the wave corresponds to the theoretical half-width of the soliton. The experimental profile becomes substantially closer to the theoretical profile with an increase in intensity ($\Delta p_e/p_0 > 2$). The large scatter of the empirical data is due to the relatively broad histogram of bubble size, the nonuniformity of the bubble distribution along the unit, and the quasisteady nature of the wave.

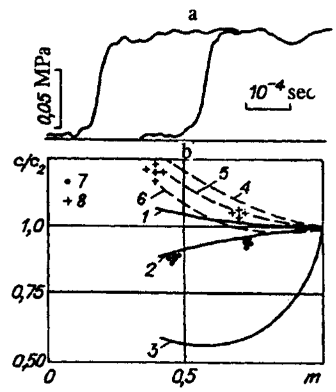

Fig. 6

Figure 5 shows experimental data on the dependence of the velocity of a shock wave in a three-phase medium on the amplitude of the wave. The parameters of the medium: the liquid — water; the gas — air; m = 0.58, φ = 0.5-2.5%. The values of velocity measured on the initial section of the wave path (points 1) agree (to within the empirical error) with the values measured a distance ~ 1 m from the point of entry to the medium (points 2). This indicates that the shock wave is formed almost instantaneously at the site of entry. The theoretical curve constructed from Eq. (6) accurately describes the experimental data within the investigated range of amplitudes. Thus, the inertial properties of the solid phase have a significant effect on the rate of wave propagation, and it is more correct to use the high-frequency velocity $c(\omega >> \omega_m)$ than the Wood velocity c_W. The velocities calculated with allowance for the coefficient expressing apparent additional mass $\left[\alpha = 1 - \frac{1}{2}\left(1 - \frac{1}{m}\right)[4]\right]$ and without allowance for this coefficient (α = 1) differ by 3% and are indistinguishable from the viewpoint of the accuracy of the velocity measurement.

Now let us examine the effect of α on the wave velocity. To improve accuracy, wave velocity was measured in a suspension of liquid with solid particles but no gas bubbles. Figure 6a shows characteristic profiles of pressure waves in a suspension of water with lead beads. The distance over which wave velocity was measured in the medium Δx = 404 mm.

Figure 6b shows the theoretical porosity dependence of sonic velocity in a suspension of water with lead (lines 1-3) and glass spheres (lines 4-6). Lines 1, 4 correspond to high-frequency sonic velocity at α = 1, lines 2 and 5 correspond to the high-frequency sonic velocity at $\alpha = 1 - \frac{1}{2}\left(1 - \frac{1}{m}\right)$ [4], and lines 3 and 6 correspond to the Wood velocity [8]. Also shown are empirical points 7 and 8 for lead and glass spheres, respectively. It is evident (especially for the lead spheres) that the experimental data is described well by the theoretical curves, which account for the effect of the apparent additional mass of the liquid on wave velocity.

REFERENCES

1. G. T. Kuster and M. N. Toksoz, "Velocity and attenuation of seismic waves in two-phase media. I-II," Geophysics, **39**, No. 5 (1974).
2. C. H. Mehta, "Scattering theory of wave propagation in a two-phase medium," Ibid., **48**, No. 10 (1983).
3. S. M. Hovem, "Viscous attenuation of sound in suspensions and high-porosity marine sediments," J. Acoust. Soc. Am., **67**, No. 5 (1980).
4. R. I. Nigmatulin, Principles of the Mechanics of Heterogeneous Media [in Russian], Nauka, Moscow (1978).
5. V. E. Nakoryakov, B. F. Pokusaev, and I. R. Shreiber, Wave Propagation in Gas– and Vapor–Liquid Media [in Russian], IT SO AN SSSR, Novosibirsk (1983).
6. V. E. Dontsov, "Structure and dynamics of finite pressure perturbations in a porous medium saturated with a liquid containing gas bubbles," Izv. Akad. Nauk SSSR Mekh. Zhidk. Gaza, No. 1 (1992).

7. V. E. Nakoryakov, V. V. Kuznetsov, and V. V. Dontsov, "Pressure waves in saturated porous media," Int. J. Mulitphase Flow, **15**, No. 6 (1979).

8. D. L. Johnson and T. S. Plona, "Slow waves and the consolidation transition," J. Acoust. Soc. Am., **72**, No. 2 (1982).